

Magneto-optical-Kerr-effect study of spin-polarized quantum-well states in a Au overlayer on a Co(0001) ultrathin film

R. Mégy, A. Bounouh, Y. Suzuki,* P. Beauvillain, P. Bruno, C. Chappert, B. Lecuyer, and P. Veillet
Institut d'Electronique Fondamentale, Université Paris Sud, 91405 Orsay Cedex, France

(Received 26 September 1994)

We have precisely measured in ultrahigh vacuum the polar magneto-optical Kerr rotation θ_K of a perpendicularly magnetized Co(0001) ultrathin film on Au(111), versus the thickness t_{Au} of a Au overlayer. Comparative measurements have been made at $\lambda = 632.8$ and 543.5 nm. At both photon wavelengths, above four atomic layers (AL's) of Au coverage we observe clear oscillations of θ_K , superimposed to the usual slow decrease with t_{Au} . While the period (around 7.7 AL's) does not change appreciably, the phase of the oscillations depends drastically on λ . Moreover, we could not detect any dependence of the oscillation parameters with the Co thickness in the range 3–6 AL's. This behavior can be interpreted as arising from strongly confined spin-polarized quantum-well states in the Au overlayer.

In ultrathin films, due to the electronic potential discontinuities experienced by electron states at interfaces, the perpendicular wave vector can be quantized, giving rise to resonances in the density of electronic states usually called quantum-well states (QWS's).¹ Those QWS's are, for instance, at the origin of the oscillating coupling observed between ferromagnetic layers through a nonmagnetic metallic spacer layer.^{2,3} Direct- and inverse-photoemission experiments allow one to directly probe QWS's in many systems such as uncovered noble-metal (100) or (111) films on ferromagnetic metals Fe or Co,^{4,5} or in a bcc Fe(100) layer on Au(100).⁶ Spectroscopic magneto-optical Kerr effect (MOKE) studies of Fe(100) on Au(100) (Refs. 7 and 8) have also been used to evidence QWS's and their dispersion in the Fe layers. More recently, it was clearly shown by photoemission experiments^{9,10} that the QWS's in a Cu(100) overlayer on Co(100) are spin polarized, as expected from theoretical predictions. As emphasized by Shoenes,¹¹ one fundamental characteristic of MOKE is that the relevant magnetization is not the total net magnetization of the layer, but the spin polarizations of the initial and final electronic states of the optical transitions involved. Moreover, MOKE is sensitive to the density of those states through the transition probability. Thus, in principle, MOKE can detect spin-polarized QWS's in a nonmagnetic layer. Oscillations of the Kerr rotation with the nonmagnetic spacer-layer thickness have indeed been observed in fcc(100)Fe/Cu/Fe (Ref. 12) or Fe(100)/(Au or Ag)/Fe (Ref. 13) trilayers, besides the coupling oscillations present in these structures. However, these two works remain incomplete, with, for instance, no study of the dependence on the ferromagnetic layer thickness, which prevents an unambiguous interpretation. Last year, we reported the existence of clear coupling oscillations in Co/Au(111)/Co trilayer structures.¹⁴ We report here the unambiguous observation by MOKE of QWS's in a Au(111) overlayer on Co(0001).

All experiments have been performed in an ultrahigh-vacuum unit with base pressure around 10^{-10} mbar (below 5×10^{-10} mbar in the sample chamber during evaporation). The unit is equipped for *in situ* reflection high-energy electron-diffraction (RHEED) and polar MOKE (PMOKE) measurements (in a field up to 3 kOe), and a precision mov-

ing shutter allows the realization of stepped wedges.^{14,15} Thicknesses are measured with a quartz monitor, calibrated against grazing x-ray measurements on thick films. We use either red ($\lambda = 632.8$ nm) or green ($\lambda = 543.5$ nm) HeNe lasers, focused to a beam diameter of about 0.4 mm (we keep all terraces about 2 mm wide in the wedges). By moving the sample with fixed laser beam we can scan the PMOKE properties of the whole sample. Note that all results discussed below have been measured on samples with a perpendicular easy magnetization axis and square PMOKE loops,¹⁵ allowing precise determination of the saturation Kerr rotation θ_K . The precision and reproducibility on the Kerr rotation have been estimated to be better than ± 0.5 mdeg.

We have studied Au/Co/Au(111) sandwich structures, grown on float-glass platelets whose backs had been carefully sanded to avoid any interference effects.¹⁶ Details on the structure of our samples have been already published.^{17,18} First a 30-nm-thick Au buffer layer is grown, then annealed to get a polycrystalline, (111) textured film, with mean lateral size of the crystallites around 200 nm. The surface is atomically flat, made of (111) terraces about 20 nm wide, separated by monoatomic steps. Co and Au layers are then grown at room temperature, using low evaporation rates (≈ 0.002 nm/s). Flat, abrupt interfaces are a prerequisite for the existence of QWS's. This is indeed true for the Au spacer layer in Co/Au/Co/Au(111) structures.¹⁴ In the Au/Co/Au(111) sandwich structure, our RHEED measurements evidence a very high quality of the Au/Co interface, smoothed by deposition of about one atomic layer (AL) of Au coverage, and a very slow increase of the roughness of the Au overlayer surface with further Au deposition.¹⁵

Several samples have been studied, with different growth sequences and thickness ranges. We shall report here results taken on two samples, that summarize best the general behavior. For sample A we have first grown a Co stepped wedge comprised of ten terraces of thicknesses $t_{\text{Co}} = 2, 3, 3.5, 4, 4.5, 5, 6, 7, 8,$ and 9 AL's. Uniform Au overlayers were then successively deposited, first by 0.5-AL steps up to a total thickness $t_{\text{Au}} = 4$ AL's, then by larger steps up to $t_{\text{Au}} = 15$ AL's. A complete PMOKE scan was performed after

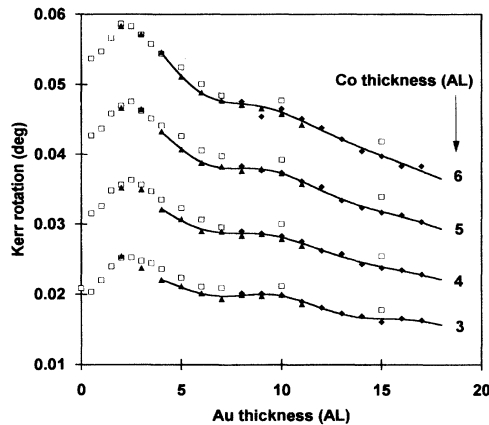


FIG. 1. Polar Kerr rotation at $\lambda = 632.8$ nm of Au/Co/Au(111) sandwiches, vs the thickness t_{Au} of the Au overlayer and for different Co thicknesses t_{Co} : squares, sample A; triangles, first series measured on sample B (2–11 AL's); diamond, second series measured on sample B (8–17 AL's). The continuous line represents the adjustment to theoretical model [Eq. (4), see text] for both series of sample B.

each deposition. Sample B was made as a double crossed stepped wedge. First a Co stepped wedge was grown, with five terraces of $t_{\text{Co}} = 3, 3.5, 4, 5$, and 6 AL's. Then a Au stepped wedge was grown perpendicularly to the first one, comprised of ten terraces of $t_{\text{Au}} = 2, 3, 4, 5, 6, 7, 8, 9, 10$, and 11 AL's. Complete PMOKE scans were then performed with both red and green lasers, followed by deposition of a uniform 6-AL-thick Au overlayer, and final PMOKE scans. The t_{Au} range extends thus by 1 AL steps from 2 to 17 AL's, with four intermediate thicknesses (8–11 AL's) doubled to check for experimental precision.

The experimental variation of θ_K versus t_{Au} is given in Fig. 1 for $t_{\text{Co}} = 3, 4, 5$, and 6 AL's of both samples. Note first that the agreement between both series measured on sample B is excellent, well within our estimated precision. Indeed, no detectable evolution occurs between the two steps of the overlayer deposition. Moreover, this confirms the good control of the thickness and uniformity of the layers. Weak (below 2 mdeg) but significant differences appear between results for samples A and B at t_{Au} above 3 AL's. They can be tentatively attributed to small structural differences induced by the very different growth sequences. In any case, *both samples display exactly the same overall behavior*, with an initial fast increase of θ_K up to a peak at $t_{\text{Au}} \approx 2.5$ AL's, followed by a slower decrease. *Most interestingly, to this decrease are superimposed clear oscillations of θ_K with t_{Au} .*

The initial increase of θ_K is probably related to the completion of the Au/Co interface and thus may result from many different origins. For instance, it has been shown that during the initial stages (1–3 AL's) of the growth of Au(111) on Co,⁵ transitory electronic features appear in the photoemission spectra. There is also some similarity between this behavior and the cusp in interface magnetic anisotropy observed on Co/noble-metal systems.^{15,19} A more detailed study is clearly necessary. In this paper we would rather concen-

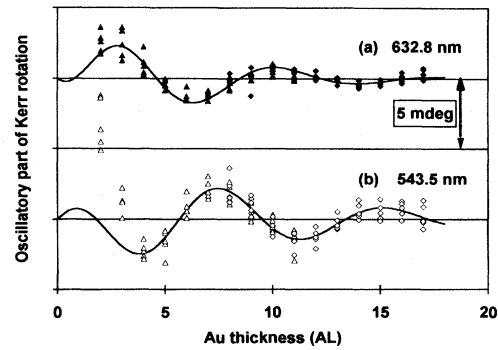


FIG. 2. Oscillatory part θ_{osc} of the variation of the polar Kerr rotation of Au/Co/Au(111) sandwiches, vs the Au overlayer thickness t_{Au} : triangles, first series measured on sample B, and diamonds, second series measured on sample B, both series for all Co thicknesses of sample B. θ_{osc} was obtained by subtracting, from the experimental value θ_K , a nonoscillating contribution θ_{opt} estimated from Eq. (1) with parameters a, b, c , and d taken from the linear fits of Fig. 3. The continuous line has been calculated from Eq. (3), using average values of the parameters α, δ, Λ , and φ in Table I.

trate on the discussion of the asymptotic behavior, i.e., the oscillating decrease at t_{Au} above 3 AL's.

The following simple considerations help to get a deeper understanding of the effect. As reported before,^{16,20,21} classical multiple-reflection calculations are able to predict the general experimental variations of θ_K in our structures. For the very low thicknesses considered here ($t/\lambda \ll 1$), all calculated variations can be fitted closely to combinations of linear functions in t_{Co} and t_{Au} .^{16,20,21} We have actually used the following expression to represent the nonoscillating experimental asymptotic behavior of Fig. 1:

$$\theta_{\text{opt}} = (at_{\text{Co}} + b)t_{\text{Au}} + ct_{\text{Co}} + d. \quad (1)$$

Note here that the necessity to introduce the constant term d in the development (1) (Refs. 16 and 20) is the signature of an interface contribution to θ_K ,^{20,21} and the initial increase with t_{Au} discussed above can be seen as the building of this contribution during the growth of the interface.

The difference between experimental θ_K and θ_{opt} , calculated for a good set of parameters a, b, c , and d , is displayed versus t_{Au} in Figs. 2(a) and 2(b), respectively, for experiments with red and green lasers. Clear oscillations come out at both wavelengths. But the most striking result is the excellent scaling of all curves for different Co thicknesses: *in the thickness range of the present work, no dependence on t_{Co} of the oscillation parameters is detectable within our experimental accuracy.* Moreover, the phase of the oscillations depends strongly on the photon energy: this confirms that we are not observing only an effect of fluctuations in t_{Au} around the estimated values.

Indeed, the observed behavior can best be explained in terms of QWS's in the Au overlayer. QW resonances are expected to modify the optical-conductivity tensor σ_{ij} of the Au overlayer. A change in the diagonal component σ_{xx} , i.e., in the nonmagnetic complex optical index n , could in principle give oscillations, through a modulated enhancement of

θ_K in a multiple-reflection scheme. Moreover, the QW resonance states can be spin polarized due to the interface with Co.^{9,10} As stressed in the beginning of the paper, they will in that case give a nondiagonal contribution σ_{xy} , and thus a direct magneto-optical contribution to θ_K .

A detailed theoretical treatment of the effect is beyond the scope of this paper, and will be published elsewhere. We shall only report here the main steps, and discuss the predictions in relation with our experimental results. The initial frame of the calculation is suggested by the validity of the linear approximation of Eq. (1). For a general stacking of N ultrathin layers of conductivity tensor $\sigma^{(j)}$ and thickness t_j (with $j=1$ for the topmost layer) on top of an infinitely thick nonmagnetic substrate ($\sigma^{(s)}, t_s$), a virtual index calculation⁷ developed at order 2 in (t_j/λ) gives the following expression for the complex Kerr rotation:

$$\theta_K + i\varepsilon_K = \sum_{j=1}^N 4\pi i \frac{\sigma_{xy}^{(j)}}{\sigma_{xx}^{(s)}} \left(\frac{t_j}{\lambda} \right) \times \left\{ 1 + 2\pi i \sqrt{1 + i\sigma_{xx}^{(s)}/\varepsilon_0\omega} \left[\left(\frac{t_j}{\lambda} \right) + 2 \sum_{k=1}^{j-1} \left(\frac{t_k}{\lambda} \right) + 2 \sum_{k=1}^N \left(\frac{\sigma_{xx}^{(k)}}{\sigma_{xx}^{(s)}} - 1 \right) \left(\frac{t_k}{\lambda} \right) \right] \right\}. \quad (2)$$

We have applied this expression to the following model stacking: Au(t_{Au})/Co(t_{Co})/interface/Au(111), where the interface layer (replacing actually the two interfaces) is here to reproduce the experimental constant term d in Eq. (1),^{16,20} and the Au(111) substrate is supposed to be infinitely thick. Although much simpler than our real samples, this model contains all relevant parameters needed to discuss our results. The linear development of Eq. (1) is then easily derived.²² In the final expression, the diagonal conductivity σ_{xx}^{Au} of the Au overlayer appears only in second-order terms in t/λ , moreover with a dominant contribution in the $(t_{Au}t_{Co}/\lambda^2)$ term, and thus cannot be at the origin of the observed oscillations. On the contrary, the leading contribution of σ_{xy}^{Au} is in the coefficient b of the term linear in t_{Au} , in agreement with the scaling behavior of Fig. 2.

A model calculation of σ_{xy}^{Au} has been made along the techniques developed for 3d transition metals ferromagnetic ultrathin films.²³ Optical transitions are assumed to occur between occupied bulk-type d states and unoccupied p states. In Au the final states are supposed to be spin polarized QWS's because of the boundary conditions with the ferromagnetic underlayer. The most general configuration gives the following expression for the oscillating contribution to parameter b of Eq. (1):

$$b_{osc} = \alpha e^{-t_{Au}/\delta} \cos\left(2\pi \frac{t_{Au}}{\Lambda} + \varphi\right), \quad (3)$$

where δ is an attenuation length related to the lifetime of excited states.

TABLE I. Parameters of the oscillatory part of the polar Kerr rotation [Eq. (3)]: λ , light wavelength; t_{Co} , Co thickness; α , amplitude; δ , attenuation length; Λ , period; φ , phase. The values have been obtained by independently fitting to Eq. (4) every variation with overlayer thickness t_{Au} , measured on sample *B* for different Co thicknesses.

λ (nm)	t_{Co} (AL)	α (mdeg/AL)	δ (AL)	Λ (AL)	φ (rad)
632.8	3	0.37	6.2	7.4	-2.2
	4	1.09	3.4	8.0	-1.9
	5	1.73	3.2	7.5	-2.4
	6	4.68	2.2	7.8	-2.4
543.5	3	1.45	4.3	7.7	0.0
	4	1.49	4.7	7.9	0.3
	5	1.70	4.5	7.7	0.1
	6	1.47	4.9	7.4	-0.2

To get the most objective test of our hypothesis, we performed, on every $\theta_K(t_{Au})$ variation measured on sample *B* for different Co thicknesses, independent least-squares fits to the expression

$$\theta_K = (m_1 + b_{osc})t_{Au} + m_2. \quad (4)$$

The quality of the fits is very good for all points with $t_{Au} \geq 4$ AL's, as can be seen in Fig. 1. Resulting values of α , δ , Λ , and φ are given in Table I, and variations of m_1 and m_2 are plotted in Fig. 3. Note first that, as expected from Eq. (1), m_1 and m_2 vary linearly with t_{Co} ($m_1 = at_{Co} + b$ and $m_2 = ct_{Co} + d$). Moreover, within our experimental precision, no significant dependence versus t_{Co} is observed for all parameters in b_{osc} , all the more for $\lambda = 543.5$ nm, for which higher values of θ_K result in a better precision. *This confirms our interpretation in terms of spin-polarized QWS's, with complete confinement in the Au overlayer.* As discussed before, the average values of φ are very different for both wavelengths (respectively, $\varphi \approx -2.2$ and $+0.2$ rad for $\lambda = 632.8$ and 543.5 nm). On the contrary, Λ keeps about the

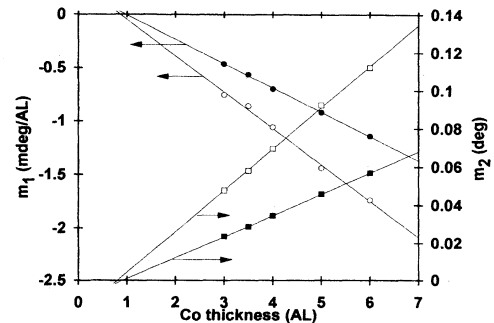


FIG. 3. Dependence vs Co thickness of the parameters m_1 and m_2 of Eq. (4), characterizing the nonoscillatory part of the polar Kerr rotation θ_K of Au/Co/Au(111) sandwiches (full symbols, $\lambda = 632.8$ nm; open symbols, $\lambda = 543.5$ nm). m_1 and m_2 have been determined by independently fitting to Eq. (4) every θ_K variation with Au overlayer thickness, measured on sample *B* for different Co thicknesses. The straight lines correspond to least-squares fits.

same value, around 7.7 AL's. According to Ref. 23, the oscillation period is given by the inverse of wave vectors caliperling (in the sense of Ref. 3) an isoenergy-difference (between initial and final states) surface. A similar period could thus come from similar surfaces, given the small photon-energy difference considered here (respectively, 1.96 and 2.28 eV). The phase depends on more subtle parameters (reflection coefficients of electronic states³).

As a conclusion, we have observed oscillations of the Kerr rotation of Au/Co/Au(111) sandwiches versus the Au overlayer thickness. Detailed analysis of our data provides strong evidence in favor of a magneto-optical contribution, induced by the existence of strongly confined spin-polarized

QWS's in the Au overlayer. Extended band calculations are in progress to identify the initial and final states.

The authors wish to thank J. Corno (Institut d'Optique, Université Paris-Sud, Orsay, France) for x-ray-calibration experiments, and gratefully acknowledge motivating discussions with J. Ferré (Laboratoire de Physique des Solides, Université Paris-Sud, Orsay, France) and S. Visnovsky (Charles University, Prague, Czech Republic) at the beginning of this work. The Institut d'Electronique Fondamentale is a research unit associated with CNRS (URA 022). This research has also been sponsored by the HCM program "Novel ultrathin films" of the European Union.

*Permanent address: National Institute for Advanced Interdisciplinary Research, 1-1-4 Higashi, Tsukubashi, Ibaraki 305, Japan.

¹M. D. Stiles, Phys. Rev. B **48**, 7238 (1993).

²D. M. Edwards, J. Mathon, R. B. Muniz, and M. S. Phan, Phys. Rev. Lett. **67**, 493 (1991).

³P. Bruno, J. Magn. Magn. Mater. **121**, 248 (1993).

⁴J. E. Ortega, F. J. Himpsel, G. J. Mankey, and R. F. Willis, Phys. Rev. B **47**, 1540 (1993).

⁵D. Hartmann, W. Weber, A. Rampe, S. Popovic, and G. Güntherodt, Phys. Rev. B **48**, 16 837 (1993).

⁶F. J. Himpsel, Phys. Rev. B **44**, 5966 (1991).

⁷Y. Suzuki, T. Katayama, S. Yoshida, K. Tanaka, and K. Sato, Phys. Rev. Lett. **68**, 3355 (1992).

⁸Y. Suzuki and T. Katayama, in *Magnetic Ultrathin Films: Multilayers and Surfaces/Interfaces and Characterization*, edited by B. T. Jonker, S. A. Chambers, R. F. C. Farrow, C. Chappert, R. Clarke, W. J. M. de Jonge, T. Egami, P. Grünberg, K. M. Krishnan, E. E. Marinero, C. Rau, and S. Tsunashima, MRS Symposia Proceedings No. 313 (Materials Research Society, Pittsburgh, 1993), p. 153.

⁹K. Garrison, Y. Chang, and P. D. Johnson, Phys. Rev. Lett. **71**, 2801 (1993).

¹⁰C. Carbone, E. Vescovo, O. Rader, W. Gudat, and W. Eberhardt, Phys. Rev. Lett. **71**, 2805 (1993).

¹¹J. Shoenes, in *Materials Science and Technology*, edited by R. W. Cahn, P. Haasen, and E. J. Kramer (VCH, Weinham, Germany, 1992), Vol. 3A, pp. 147-255.

¹²W. R. Bennett, W. Schwarzacher, and W. F. Egelhof, Jr., Phys. Rev. Lett. **65**, 3169 (1990).

¹³T. Katayama, Y. Suzuki, M. Hayashi, and A. Thiaville, J. Magn. Magn. Mater. **126**, 527 (1993).

¹⁴V. Grolier, D. Renard, B. Bartenlian, P. Beauvillain, C. Chappert, C. Dupas, J. Ferré, M. Galtier, E. Kolb, M. Mulloy, J. P. Renard, and P. Veillet, Phys. Rev. Lett. **71**, 3023 (1993).

¹⁵S. Ould-Mahfoud, R. Mégy, N. Bardou, B. Bartenlian, P. Beauvillain, C. Chappert, J. Corno, B. Lecuyer, G. Sczigel, P. Veillet, and D. Weller, in *Magnetic Ultrathin Films: Multilayers and Surfaces/Interfaces and Characterization* (Ref. 8), p. 251.

¹⁶S. Visnovsky, M. Nyvlt, V. Prosser, J. Ferré, G. Pénissard, D. Renard, and G. Sczigel, J. Magn. Magn. Mater. **128**, 179 (1993).

¹⁷D. Renard and G. Nihoul, Philos. Mag. B **55**, 75 (1987).

¹⁸C. Cesari, J. P. Faure, G. Nihoul, K. Le Dang, P. Veillet, and D. Renard, J. Magn. Magn. Mater. **78**, 296 (1989).

¹⁹B. N. Engel, M. H. Wiedmann, R. A. Van Leeuwen, and C. M. Falco, Phys. Rev. B **48**, 9894 (1993).

²⁰M. Nyvlt, V. Prosser, S. Visnovsky, J. Ferré, D. Renard, and R. Krishnan, J. Magn. Magn. Mater. (to be published).

²¹P. Beauvillain, A. Bounouh, C. Chappert, R. Mégy, and P. Veillet, J. Magn. Magn. Mater. (to be published).

²²A more detailed analysis allows one to predict also the experimental orders of magnitude for the parameters a , b , c , and d . There is, for instance, a negligible t_{Au}^2 term, and a t_{Co}^2 term that we cannot, however, expect to detect given our very narrow range of t_{Co} .

²³Y. Suzuki and P. Bruno, J. Magn. Magn. Mater. (to be published).